ERDC/CRREL MP-21-17

US Army Corps
of Engineers®
Engineer Research and
Development Center

Reproducibility Assessment and Uncertainty Quantification in Subjective Dust Source Mapping

Samantha N. Sinclair and Sandra L. LeGrand

August 2021

Cold Regions Research and Engineering Laboratory

The U.S. Army Engineer Research and Development Center (ERDC) solves the nation's toughest engineering and environmental challenges. ERDC develops innovative solutions in civil and military engineering, geospatial sciences, water resources, and environmental sciences for the Army, the Department of Defense, civilian agencies, and our nation's public good. Find out more at www.erdc.usace.army.mil.

To search for other technical reports published by ERDC, visit the ERDC online library at https://erdclibrary.on.worldcat.org/discovery.

ERDC/CRREL MP-21-17
August 2021

Reproducibility Assessment and Uncertainty Quantification in Subjective Dust Source Mapping

Samantha N. Sinclair and Sandra L. LeGrand

Cold Regions Research and Engineering Laboratory
U.S. Army Engineer Research and Development Center
72 Lyme Road
Hanover, NH 03755

Final report

Prepared for Assistant Secretary of the Army for Acquisition, Logistics, and Technology (ASA-ALT)
Washington, DC 20314

Under ARTEMIS STO-R and DUST-CLOUD Applied Science Research Programs

Preface

This study was conducted for the Assistant Secretary of the Army for Acquisition, Logistics, and Technology (ASA-ALT) and funding support was provided by the U.S. Army Terrestrial Environmental Modeling & Intelligence System Science Technology Objective–Research (ARTEMIS STO-R) 053HJO/FAN U4357509, "Dynamic Undisturbed Soils Testbed to Characterize Local Origins and Uncertainties of Dust (DUST-CLOUD)" and the "Forecasting EO/IR Extinction Characteristics for Active and Passive Optical Systems" H407HL/FAN U4365035 applied science research programs.

The work was performed by the Army's Engineer Research and Development Center, Cold Regions Research and Engineering Laboratory (ERDC-CRREL). At the time of publication of this paper, the Deputy Director of ERDC-CRREL was Mr. David Ringelberg and the Director was Dr. Joseph Corriveau.

This article was originally published online in *Aeolian Research* on 24 June 2019.

We thank Mr. Bruce Elder, Mr. Michael Morgan, Mr. Ross Alter, Mr. Christopher Felt, Ms. Ashley Mossell, and Ms. Taylor Hodgdon for assistance with plume head mapping and labeling, Mr. Ricardo Vera and Mr. John Fegyveresi for assistance with data processing, and Mr. David Ringelberg and Mr. Nicholas Webb for thoughtful discussions, input, and editing.

The Commander of ERDC was COL Teresa A. Schlosser and the Director was Dr. David W. Pittman.

Reproducibility assessment and uncertainty quantification in subjective dust source mapping

ABSTRACT

Accurate dust-source characterizations are critical for effectively modeling dust storms. A previous study developed an approach to manually map dust plume-head point sources in a geographic information system (GIS) framework using Moderate Resolution Imaging Spectroradiometer (MODIS) imagery processed through dust-enhancement algorithms. With this technique, the location of a dust source is digitized and recorded if an analyst observes an unobscured plume head in the imagery. Because airborne dust must be sufficiently elevated for overland dust-enhancement algorithms to work, this technique may include up to 10 km in digitized dust-source location error due to downwind advection. However, the potential for error in this method due to analyst subjectivity has never been formally quantified. In this study, we evaluate a version of the methodology adapted to better enable reproducibility assessments amongst multiple analysts to determine the role of analyst subjectivity on recorded dust source location error. Four analysts individually mapped dust plumes in Southwest Asia and Northwest Africa using five years of MODIS imagery collected from 15 May to 31 August. A plume-source location is considered reproducible if the maximum distance between the analyst point-source markers for a single plume is $\leq$10 km. Results suggest analyst marker placement is reproducible; however, additional analyst subjectivity-induced error (7 km determined in this study) should be considered to fully characterize locational uncertainty. Additionally, most of the identified plume heads (> 90%) were not marked by all participating analysts, which indicates dust source maps generated using this technique may differ substantially between users.

1. Introduction

Airborne mineral dust influences global climate patterns and biogeochemical processes (e.g., Mahowald et al., 2005, 2010, 2014; Ravi et al., 2011; Webb et al., 2012; Boucher et al., 2013). Furthermore, hazardous air quality conditions created by dust can negatively affect human health, agriculture, visibility, and communication on regional and local scales (Rushing et al., 2005; De Longueville et al., 2010; Okin et al., 2011; Sprigg et al., 2014; Al-Hemoud et al., 2017; Middleton and Kang, 2017). While considerable advances have been made in dust event simulation and hazard mitigation (e.g., Knippertz and Stuut, 2014; Shepherd et al., 2016), the processes controlling the spatial and temporal variability of dust emissions (e.g., microscale momentum transfer processes, integrated effects of soil state and composition on erodible material availability, etc.) are not fully understood (Richter and Gill, 2018).

Resolving these governing mechanisms continues to be a challenge, largely because comprehensive *in situ* dust emission flux measurements are difficult to acquire (Shinoda et al., 2011; Webb et al., 2016). Several efforts have been made to characterize dust emission provenance and activity through remote sensing (e.g., Prospero et al., 2002; Miller, 2003; Bullard et al., 2008; Koven and Fung, 2008; Baddock et al., 2009; Lee et al., 2009; Walker et al., 2009; Ginoux et al., 2012; Muhs et al., 2014; Jafari and Malekian, 2015; Moridnejad et al., 2015; Miller et al., 2017; Feuerstein and Schepanski, 2018; Hennen et al., 2019; Yu et al., 2019). Over the past two decades, these satellite-based approaches have enabled a deeper understanding of global dust distributions, emission patterns, and variability over time (e.g., Richter and Gill, 2018). For a more comprehensive overview and chronology of satellite-based dust survey advancements, see Walker et al. (2009) and Chiapello (2014).

A semi-automated technique pioneered by Walker et al. (2009; W09 henceforth) is widely utilized to remotely identify active dust sources over regional scales, particularly in the operational forecasting sector. In the W09 approach, an analyst manually examines dust-enhanced false color (DEFC) satellite imagery, reported weather observations, and static terrain data in a geographic information system (GIS) framework. If an unobscured dust plume head is observed, its location and attributes of interest are recorded in a master vector-based dataset of active dust sources. In instances where the imagery shows dust clouds emanating from broad swaths, a closed curve is drawn to best fit the edge of the head of the dust cloud. This approach does not have a dependency on a particular imagery dataset;

however, high-resolution (1 km or finer) imagery is preferred to adequately resolve small point-source plumes (1–10 km across) that tend to comprise synoptic and mesoscale dust events (those on the order of 5–100 km across). W09 utilized 1 km grid-scale imagery derived from the Moderate Resolution Imaging Spectroradiometer (MODIS) instrument on the Terra and Aqua satellites. Although W09 records dust source locations with 1 km precision, the authors note the potential for locational error due to limitations of DEFC algorithms over barren and sparsely vegetated landscapes. In general, these algorithms require airborne dust to be sufficiently elevated above the land surface to discern thermal and reflectance contrast signals. As such, W09 suggests that dust source datasets generated from 1 km MODIS imagery may include location errors of up to 10 km. In other words, the actual eroding dust sources on the surface are located up to 10 km away from the elevated plume-head point sources observed in the imagery due to downwind advection prior to satellite detection (i.e., advection error).

The W09 technique is often used for parameterizing sources of dust in regional-scale weather forecasting models, such as the U.S. Navy's operational Coupled Ocean/Atmosphere Mesoscale Prediction System (COAMPS) model (e.g., Liu et al., 2007; Ault et al., 2011), and as a proxy for observations of active dust source emissions (e.g., Lary et al., 2016). To our knowledge, however, the potential for location error in the W09 method due to analyst subjectivity has never been formally assessed or quantified. We define subjectivity here as the level of variability expected in plume-head marker location caused by changing the person conducting the mapping exercise to a different individual (assuming all participating analysts receive the same procedural training and follow the same method for choosing their marker placement).

Sinclair and Jones (2017) conducted an exploratory study to investigate the role of analyst subjectivity on the reproducibility of dust source datasets created using a modified version of the W09 methodology. In the Sinclair and Jones (2017) approach, analysts place a single point at the location of an unobscured plume head, rather than outlining the plume head with a curve, in order to simplify comparisons between datasets produced by different analysts. Plumes emanating from broad swaths instead of discernable point sources were ignored.

For the Sinclair and Jones (2017) study, multiple analysts independently mapped active dust plumes for two dust event case studies using 1 km grid-scale DEFC MODIS imagery and the modified W09 approach. Mapped plume-head point sources were considered reproducible if the maximum distance between the analysts' dust source markers did not exceed 10 km. Sinclair and Jones (2017) found that by increasing the tolerance for location error from 10 km to 15 km, dust-source dataset reproducibility increased substantially (from 28% up to 85% in one case study), suggesting analyst subjectivity may have a notable effect on dust-source location error.

The goal of this study is to expand upon the Sinclair and Jones (2017) assessment through a more robust and comprehensive reproducibility investigation of the modified W09 technique. Four analysts independently examined five concurrent years of late spring and summertime MODIS satellite imagery of Southwest Asia and Northwest Africa and cataloged their interpretations of active dust source locations. The four analysts also documented their level of certainty in their choice of marker placement each time they recorded a point. These datasets were then compared to evaluate the role of analyst subjectivity and marker placement confidence on plume head marker location error.

2. Study region

To mirror the W09 study as closely as possible, the same study area in Southwest Asia was chosen for this work. The study area includes 30 countries across Southwest Asia and Northeast Africa and comprises almost all of the Middle East (Fig. 1). The greatest concentration of dust sources in the Middle East are observed at the border between Syria and Iraq along the Tigris and Euphrates Rivers (see Fig. 1; Moridnejad et al., 2015; Parolari et al., 2016). A high concentration of dust storms also occur at the convergence between the borders of Iran, Pakistan, and Afghanistan where dust sources are located in valleys between mountain ridges (Middleton, 1986). Geomorphic landforms in the area with high dust emission potential include alluvial fans and ephemeral lakes, such as the Hamun dry lakes and the deltaic fan associated with the Helmand River (see Fig. 1; Goudie and Middleton, 2006). Dense dust plumes originating from these sources are transported by strong northwesterly winds blowing through lowland areas. The onset of these strong, seasonal winds is known as the summer Shamal season, which occurs in the late spring through summer (Yu et al., 2016; Bou Karam Francis et al., 2017). To coincide with the summer Shamal, satellite imagery evaluated in this study were generated using five years (2012–2016) of MODIS data collected from 15 May to 31 August.

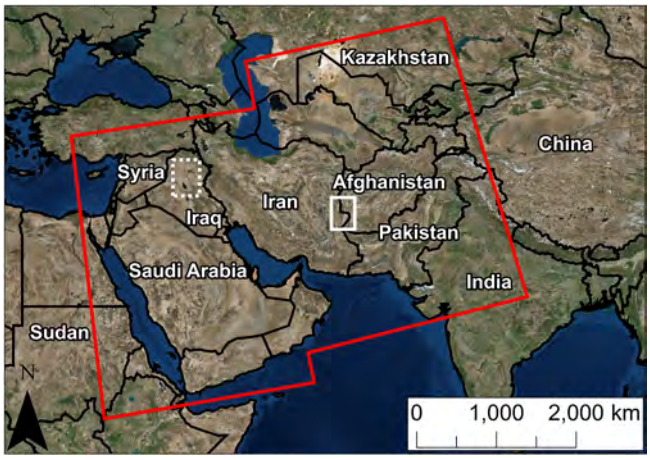

Fig. 1. A map depicting the portion of Southwest Asia and Northeast Africa examined in this study. The red polygon outlines the region for which MODIS imagery was downloaded. The solid and dashed white boxes show the location of the Hamun dry lakes and a portion of the Tigris and Euphrates Rivers, respectively. (For interpretation of the references to color in this figure legend, the reader is referred to the web version of this article.)

3. Methods

To examine the role of user subjectivity, four analysts independently mapped dust plume-head point sources from MODIS imagery following the procedures outlined in Sinclair and Jones (2017). The methodology used here differs from the original W09 technique in that 1) analysts place a single point at the location of an unobscured plume head, rather than outlining the plume head with a curve, and 2) analysts assign each mapped point a quality score (confidence level in marker placement) on a qualitative scale of 1–3, where 3 is the most confident and 1 is the least confident. As discussed in Sinclair and Jones (2017), quality scores are intended as a means to communicate user confidence in plume-head mapping decisions and are highly subjective. Users assigned a particular point a quality score of 3 only when they were confident in the placement of the point and felt certain dust was originating from that location. A quality score of 2 meant users were almost certain dust was coming from that location but were not entirely confident. A quality score of 1 meant the user had a low level of confidence in the placement of their point.

Plumes emanating from a broad swath instead of a discernable point source were not considered for this analysis. True-color and DEFC imagery were downloaded and processed, and usable images were selected based on a perceived potential for mappable sources. Plume-head point sources were mapped using ArcMap 10.3 and assigned quality scores. Results were aggregated and assessed for reproducibility. A mapped plume-head point source was considered reproducible if the maximum distance between point-source markers placed by the four analysts for a single plume was ≤ 10 km, a limit defined by the potential for advection error when using the original W09 methodology.

3.1. MODIS imagery

Satellite images were derived from MODIS data, which have been collected by the Earth Observing System Terra and Aqua satellites since late-1999 and mid-2002, respectively. MODIS Level 1B 1 km Calibrated Radiance granules for the region outlined in Fig. 1 were downloaded following the procedures in Sinclair and Jones (2017). Note, in the Sinclair and Jones (2017) study, Automated Surface Observing Systems (ASOS) weather station data were used to guide MODIS image downloads, as only imagery associated with weather reports that depicted "dusty" conditions were downloaded. In our study, however, all available MODIS imagery from 15 May to 31 August of 2012 through 2016 were downloaded to ensure dust events were not missed. A single analyst manually sorted through the five years of imagery, removed images where satellite pass over coverage was insufficient or only clear conditions were present, selected all instances where lofted dust was clearly depicted, and provided the images to the team of analysts for mapping.

Three unique images were generated from each acquired granule. The first was a true-color image, a bird's eye representation of Earth from space (Fig. 2A). The other two images were created using DEFC algorithms (Fig. 2B and C). The first of the dust-enhanced images was rendered using a technique described by Miller (2003), which uses visible, near-infrared, thermal-infrared, and water–vapor channels to distinguish elevated dust from the underlying background. Lofted dust appears pink, landscapes have blue and green hues, water and steep terrain are red, and clouds appear aqua (Fig. 2B).

The second dust-enhanced image was generated using an algorithm developed by the European Organization for the Exploitation of Meteorological Satellites (EUMETSAT) for use with their geostationary satellite data, which has since been adapted for other satellite platforms (e.g., Lensky and Rosenfeld, 2008; Brindley et al., 2012). Unlike the Miller (2003) approach, the EUMETSAT technique does not require the use of visible channels, which makes it useful for both day and nighttime dust detection. Lofted dust appears pink against purple landscapes, and thick clouds appear red, which in some instances can camouflage the dust (Fig. 2C). Imagery created with true-color settings, the Miller (2003) algorithm, and the EUMETSAT algorithm are labeled "True Color," "MILLER," and "EUMETSAT," respectively, throughout this paper.

Originally created by Lee et al. (2009) and since adopted by others (e.g., Hahnenberger and Nicoll, 2014), some previous studies have used 250 m resolution True Color MODIS imagery with the W09 methodology in place of the 1 km True Color and dust enhanced imagery

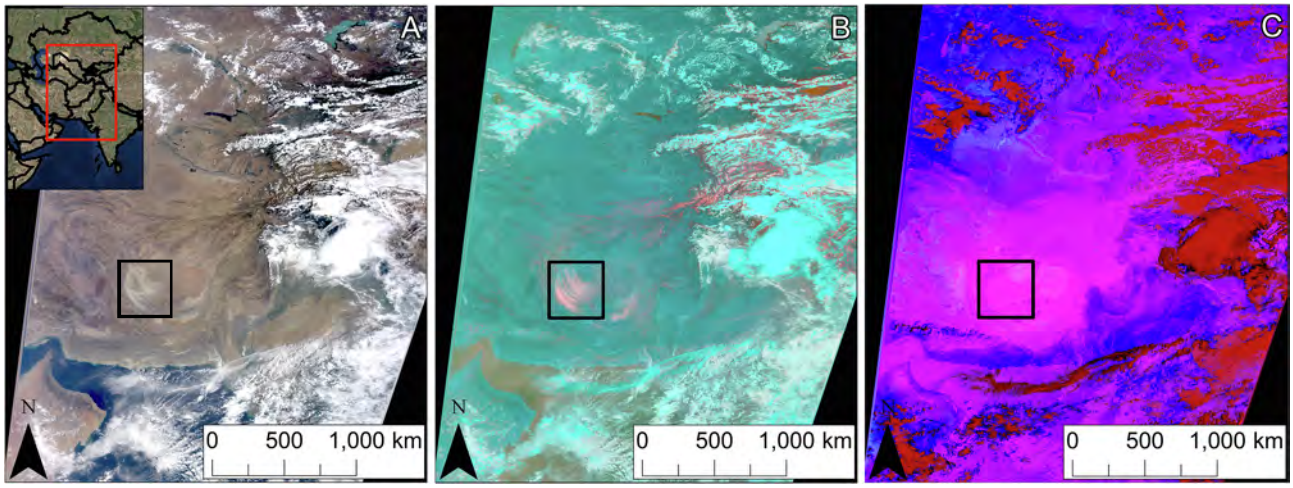

Fig. 2. MODIS satellite imagery of Southwest Asia. Panels A, B, and C represent the area outlined by the red box within the inset of Panel A. Panel A is a True Color image that depicts white clouds against a brown landscape; a bird's eye representation of Earth. Panel B is a MILLER image that shows aqua colored clouds against a blue/green landscape. Lofted dust appears pink while high-relief topography appears red. Panel C is an EUMETSAT image that displays red clouds against a purple/blue landscape. Lofted dust appears pink. The black box shown in each panel depicts a dust storm that occurred on July 9, 2013 at 0610 UTC at the borders between Iran, Afghanistan, and Pakistan. (For interpretation of the references to color in this figure legend, the reader is referred to the web version of this article.)

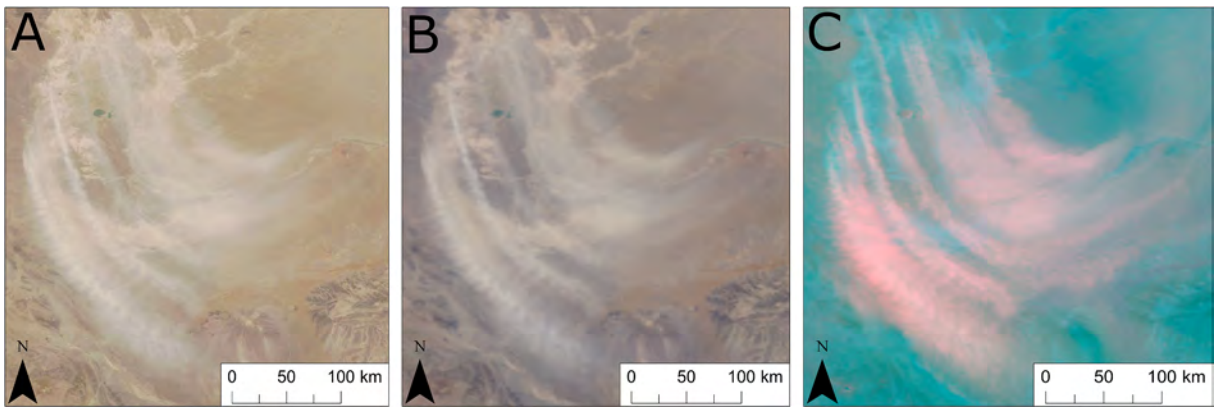

Fig. 3. MODIS imagery of a dust storm that occurred on July 9, 2013 at 0610 UTC at the borders between Iran, Afghanistan, and Pakistan. The extent of each panel is depicted by the black box in Fig. 2. Panel A: 250 m resolution True Color image. Panel B: 1 km resolution True Color image. Panel C: 1 km resolution MILLER image. Note that the plume-head point sources are most easily identifiable in the MILLER image. (For interpretation of the references to color in this figure legend, the reader is referred to the web version of this article.)

discussed above. We chose to use the 1 km imagery for this study for several reasons: (1) while 250 m resolution True Color imagery provides a more precise representation of the ground surface, it does not improve dust source location identification. This is because the dust still needs to be sufficiently lofted for satellite detection, and therefore plumes seen in the imagery have likely already advected downwind from their original point source, (2) the 1 km MILLER and EUMETSAT imagery reveal plume sources that would otherwise go unnoticed if only True Color imagery was utilized (Fig. 3), and (3) the goal of this study is to assess the reproducibility of and uncertainty in the original W09 methodology. To do this, we followed the original study as closely as possible, which utilized 1 km MODIS imagery.

3.2. Plume head mapping and labeling

Analysts with backgrounds in geology, meteorology, and geomorphology conducted the plume head mapping and labeling. One of the four analysts who had prior experience using the W09 methodology was tasked at training the other analysts to ensure there was consistency in mapping procedures across the team. Once the actual mapping began, however, the analysts were prohibited from collaborating to eliminate any potential persuasion or bias.

Thousands of plume-head point-source markers were generated for each year, and attributes associated with the points (e.g., latitude, longitude, granule date, granule time, quality score, and analyst number) were combined into a master data table. All three MODIS image types (True Color, MILLER, and EUMETSAT) were utilized in the mapping process. The analysts primarily relied on the MILLER images to initially locate plume-head point sources, particularly as lofted dust is most easily identifiable in these images. Once the location of a potential plume-head point source was observed, the analysts used True Color images to ensure the point was in fact lofted mineral dust, and not associated with a forest fire or thin, translucent clouds (which can also look like plume heads). The EUMETSAT images were used as supplemental/additional information to confirm the actual location of the point source. After reviewing all three image types, the analysts mapped the actual point sources against the MILLER images.

To provide a means of associating points from individual analysts to commonly perceived plumes, two additional analysts, who did not participate in the mapping stage, reviewed the data to assign dust plume identifier codes (referred to here as ID codes). To create the ID codes, the two third-party analysts examined mapped points affiliated with individual MODIS granules in ArcGIS using MILLER imagery for guidance and mapped their own collection of points anywhere they viewed a single point or cluster of points associated with a particular plume (e.g., Fig. 4). Because this approach requires some subjectivity

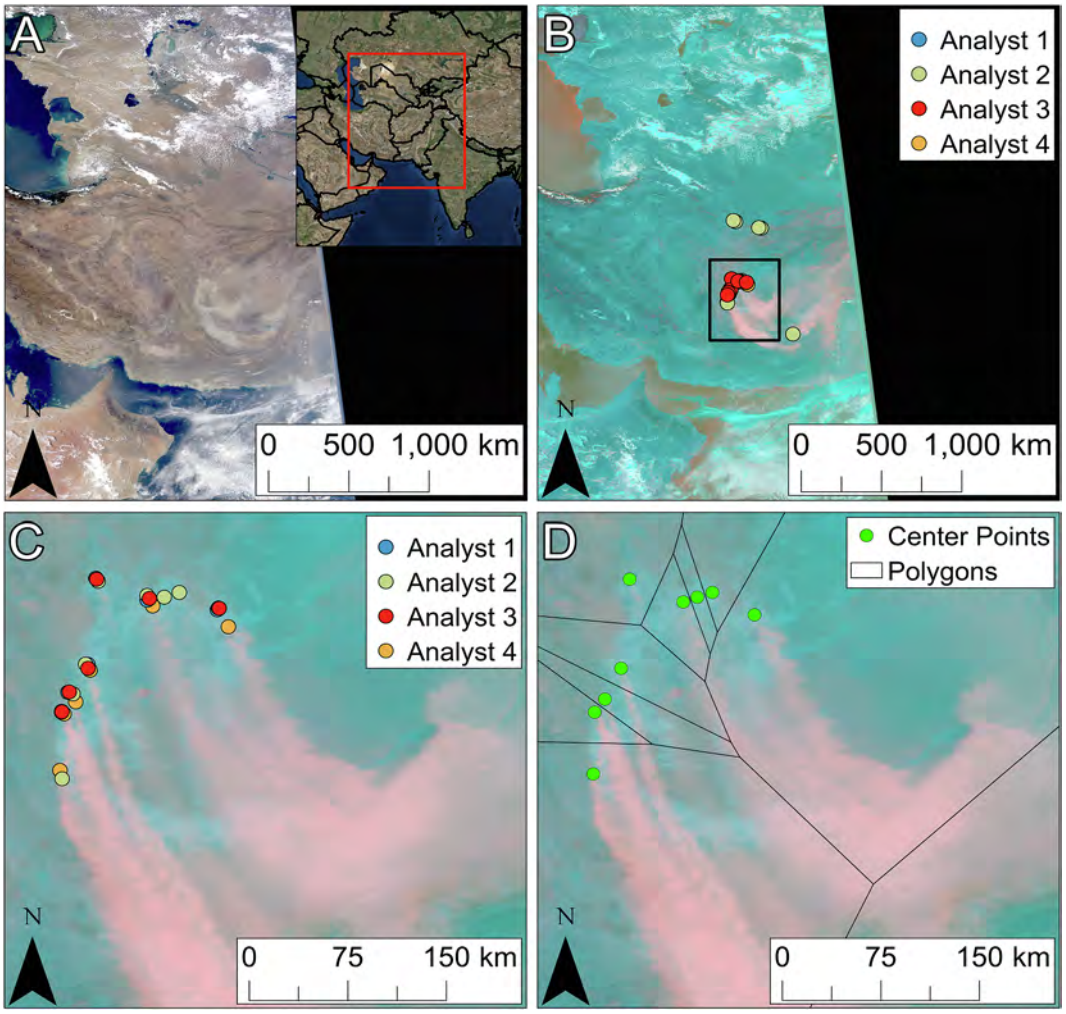

Fig. 4. MODIS imagery of a dust storm that occurred on July 9, 2013 at 0925 UTC at the borders between Iran, Afghanistan, and Pakistan. Panels A and B represent the area outlined by the red box shown in the inset of Panel A. Panel A: True Color image. Panel B: MILLER image depicting points mapped by all four analysts. Panel C: A zoomed in view of the area outlined by the black box in Panel B. Panel D: The same extent shown in Panel C and a depiction of the center points that replaced points mapped by all analysts. The polygonal division of these points used to generate unique IDs is also displayed. (For interpretation of the references to color in this figure legend, the reader is referred to the web version of this article.)

on the part of the third-party analysts, the analysts who participated in the original mapping exercise periodically reviewed plume association assessments for their respective points. A series of polygons were then generated for each granule domain with one third-party analyst point allowed per polygon (e.g. Fig. 4D). A unique ID code was then assigned to each polygon and their associated points, and a new column containing these ID codes was added to the master data table.

3.3. Limitations

Due to a general lack of *in situ* dust-emission observations, there is no way to definitively corroborate the precise locations of historically emitting dust sources on a regional scale or to verify that point sources subjectively identified by an analyst are actually true sources. Thus, quantitative assessment is limited in nature to point-placement reproducibility amongst analysts. In other words, this paper addresses the sensitivity of plume-head location placement to analyst interpretation. It does not attempt to quantify the ability of individual group members to reproduce actual emission-source patterns.

3.4. Reproducibility assessments

Following the approach used by Sinclair and Jones (2017), a digitized plume-source location is considered reproducible if the maximum distance between analyst point-source markers for a single plume is ≤10 km (Fig. 5). Linear distances between points were measured if two or more analysts identified a common plume (i.e., two or more master data table entries shared a common ID code). If three or more analysts identified the same plume, the maximum distance between the points was recorded (see Fig. 4).

We conducted six unique reproducibility assessments. The first assessment (Test 1) examined plume-head point sources that were mapped by all four analysts regardless of quality score. The other five reproducibility tests were conducted to determine if other parameters, such as quality score or the number of analysts who mapped a particular plume, influenced reproducibility. We defined each test by the number of analysts who mapped a plume head and the associated quality scores as follows: plume heads mapped by two or more analysts regardless of quality score (Test 2); plume heads mapped by two or more analysts with the highest quality score (Test 3); plume heads mapped by all four analysts with the highest quality score (Test 4); plume heads mapped by two or more analysts with the lowest quality scores excluded (Test 5); and plume heads mapped by all four analysts with the lowest quality scores excluded (Test 6) (see Table 1). The mean, median, standard deviation, maximum distance, and number of plume heads in each scenario were calculated, and test results were plotted as histograms. Results from Test 1 are likely the most representative of W09 technique reproducibility, as quality scores were not included in the original W09 methodology.

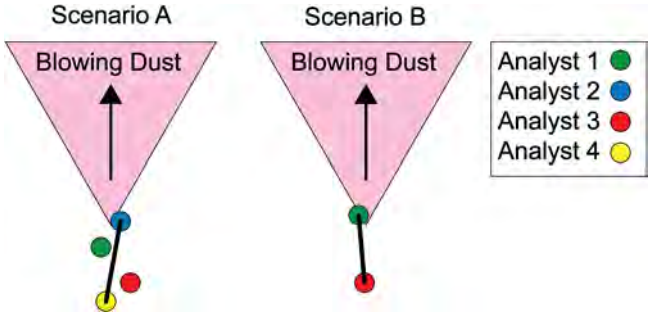

Fig. 5. Schematic diagram of the method used to identify the maximum distance between analyst markers for a common plume. Scenario A depicts a plume mapped by all four analysts, while Scenario B depicts a plume mapped by two analysts. The black line in both scenarios highlights the maximum distance between analyst points. Maximum distances were calculated in all instances a plume was mapped by two or more analysts.

4. Results

4.1. Lofted dust in MODIS imagery

Of the thousands of MODIS images downloaded for this study, only several hundred were useful for mapping plume-head point sources. This was for a variety of reasons, including: no satellite coverage during the time of a dust storm; cloud obscuration; and the occurrence of a low-concentration, short-lived, insufficiently lofted, or nighttime dust storm. Additionally, in many instances, analysts were not able to map lofted dust as it appeared as an effusive cloud without a discernable source.

During the imagery selection process, it was determined thin clouds, forest fires, and high-relief ridges also look like plume heads in the DEFC MODIS images. To eliminate these potential false positives, smoke originating in forested terrains, narrow mountain ridges, and thin clouds identified in True Color images were ruled out.

4.2. Plume head mapping results

The four analysts mapped a combined 23,380 plume-head point sources throughout the five years of MODIS imagery that were examined (Fig. 6). Of these, 39.8% were assigned a quality score of 2, 32.2% a quality score of 1, and 28% a quality score of 3. The quality scores were heterogeneously distributed across the region, and no apparent spatial or linear patterns were observed. In several cases, however, smaller (< 100 km across) areas that had a dense population of mapped plume-head point sources contained a greater abundance of plumes that had been assigned a quality score of 3 (Fig. 7).

More than 60% of all plume-head markers were mapped in Syria, Iraq, Sudan, and at the borders between Afghanistan, Pakistan, and Iran (see Fig. 6). The number of plume heads identified by each analyst varied; Analyst 1 mapped the most points (8,325) while Analyst 3 mapped the least (3,860) (Table 2). The greatest number of plume-head

Table 1
The defining criteria and results of the six reproducibility tests.

Test	Number of Analysts	Quality Scores	Number of Plumes	Median Maximum Distance (km)	Mean Maximum Distance (km)	Maximum Distance Standard Deviation (km)	Largest Maximum Distance (km)
1	4	1, 2, 3	913	7	10.4	11.2	106
2	2+	1, 2, 3	5498	5	8.8	11.6	179
3	2+	3	1401	4	5.8	6.8	63
4	4	3	120	5	6.3	5.6	33
5	2+	2, 3	3797	4	7.1	9.6	167
6	4	2, 3	516	6	8.8	9	76

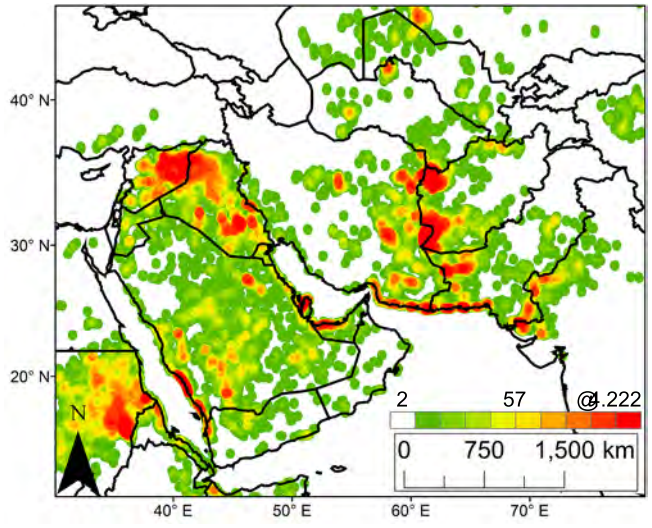

Fig. 6. Map of Southwest Asia and Northeast Africa depicting the distribution of plume-head point-source markers placed by the four analysts over the 15 May to 31 August 2012–2016 mapping period. (For interpretation of the references to color in this figure legend, the reader is referred to the web version of this article.)

markers were placed in 2012 (5,997) while the least were placed in 2016 (3,468) (Table 2). That said, 2012 had the lowest percentage of plume-head markers that were assigned a quality score of 3 (25%) and the highest percentage that were assigned a quality score of 1 (33.4%) of any year, while the opposite was true for 2016.

Out of all the plume-head markers that were identified, < 10% were mapped by all four analysts. We calculated the number of instances a single analyst was the only one within the team that did not map a particular plume-head (Table 3). Results show each analyst omitted at least 214 plume heads that the rest of the team identified. Additionally, all instances where a single analyst was the only person to map a particular plume were calculated (Table 4). Each analyst mapped between 855 and 3,990 plumes that no other team member identified. In total, 9,017 plumes (or 38% of the entire dataset) were mapped by a single analyst. Of these, however, 47% were assigned a quality score of 1, and only 15% were assigned a quality score of 3.

Table 2
Summary of all plume-head point sources identified by the four analysts within the five years of MODIS imagery. Mapped points are broken down by year and quality score for each analyst and displayed as percentages. The total number of points mapped by each analyst are also listed.

	Mapped Points	2012	2013	2014	2015	2016	Percent of Total
Analyst 1	Q1	48	42	32	21	29	37
	Q2	32	34	36	36	30	34
	Q3	20	24	32	43	41	29
	Percent of Total	29	27	19	12	13	Total Points: 8325
Analyst 2	Q1	19	12	32	38	33	25
	Q2	59	66	52	47	50	56
	Q3	22	22	16	15	17	19
	Percent of Total	33	20	13	21	13	Total Points: 6143
Analyst 3	Q1	16	17	20	26	22	21
	Q2	35	39	42	47	44	42
	Q3	49	44	38	27	34	37
	Percent of Total	16	20	14	29	21	Total Points: 3860
Analyst 4	Q1	40	44	39	42	40	41
	Q2	32	28	26	28	30	28
	Q3	28	28	35	30	30	31
	Percent of Total	17	21	19	26	17	Total Points: 5052
All Analysts	Q1	33	31	33	33	31	32
	Q2	42	42	37	39	38	40
	Q3	25	27	30	28	31	28
	Percent of Total	26	23	17	19	15	Total Points: 23,380

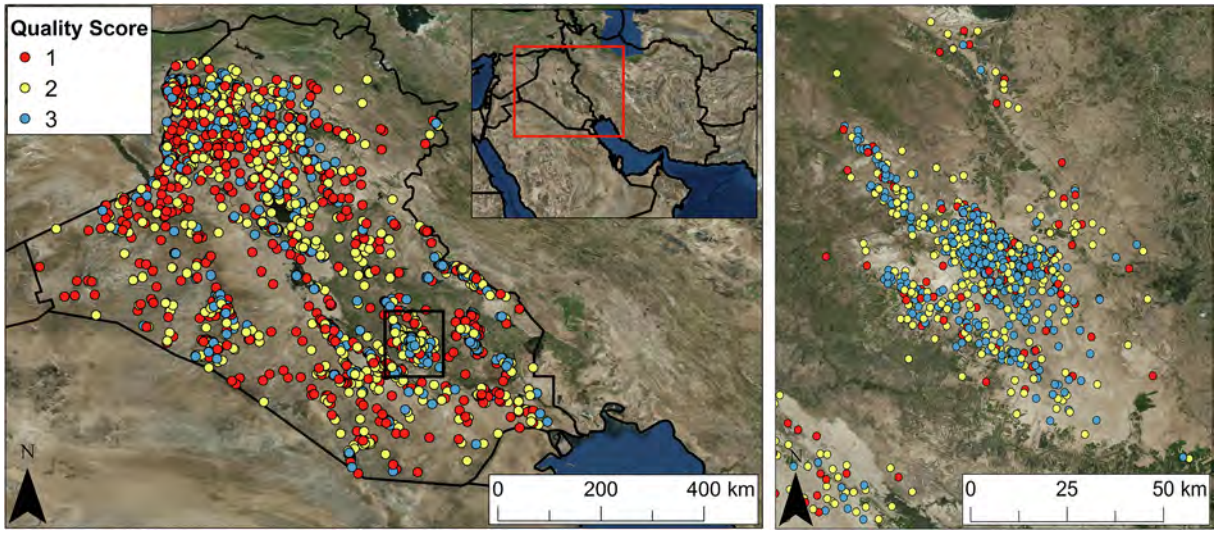

Fig. 7. Left: Plume-head markers in Iraq that were mapped by the four analysts and sorted by quality score. Regional context of this area is shown in the top right. The black box is enlarged on the Right: Highly populated area of plume-head markers. Note the majority of these points were assigned a quality score of 3. (For interpretation of the references to color in this figure legend, the reader is referred to the web version of this article.)

Table 3
Every instance a single analyst was the only one within the group that did not map a particular plume head.

	2012	2013	2014	2015	2016	Total
Analyst 1	21	27	24	100	42	214
Analyst 2	20	46	50	87	50	253
Analyst 3	227	146	80	45	33	531
Analyst 4	173	128	63	102	77	543

Table 4
Plume-head point sources that were mapped by only one analyst per year and the associated quality scores assigned to those points. The total number of plume heads each analyst was the only one to map and the percent of those points that were assigned a quality score of 1, 2 or 3 are also shown.

	Total Points	Quality Score	2012	2013	2014	2015	2016	Percent
Analyst 1	3990	Q1	751	699	390	118	215	55
		Q2	295	356	314	145	169	32
		Q3	97	89	161	91	100	13
Analyst 2	2165	Q1	220	64	72	258	154	36
		Q2	467	229	118	245	152	56
		Q3	87	26	15	29	25	8
Analyst 3	855	Q1	19	22	23	119	67	29
		Q2	37	57	37	156	114	47
		Q3	44	40	32	41	47	24
Analyst 4	2007	Q1	113	208	199	321	211	52
		Q2	78	76	103	188	110	28
		Q3	36	66	99	125	74	20
All Analysts	9017	Q1	1103	993	684	816	647	47
		Q2	877	718	572	734	545	38
		Q3	264	221	307	286	246	15

4.3. Reproducibility test results

The results from reproducibility tests 1–6 are plotted as histograms in Fig. 8. As the data does not fit a Gaussian curve, the median, rather than the mean, maximum distance between analyst plume-head markers was examined to assess reproducibility. Results from all tests produced similarly distributed, left-skewed data, as shown in Fig. 8. The primary difference between the six histograms is the sample size, or number of plume heads that fit the criteria of each test, and the maximum distance between analyst points. For example, Test 4, which required identification by all four analysts and the highest quality score, had a sample size of 120 plumes and a maximum location discrepancy of 30 km for a single plume, while Test 2, which only required identification by 2 or more analysts, had a sample size of 5,498 plumes and a maximum location discrepancy of 179 km for a single plume.

Median values of the maximum distances between analyst markers in Tests 1–6 are as follows: 7 km, 5 km, 4 km, 5 km, 4 km, and 6 km, respectively. The maximum distance between plume-head point markers ranged from < 1 km to 179 km. Surprisingly large distance outliers were double checked and confirmed accurate (in other words, they were not mislabeled points). These occasional large discrepancies were primarily due to uncommonly pronounced differences in the intensity

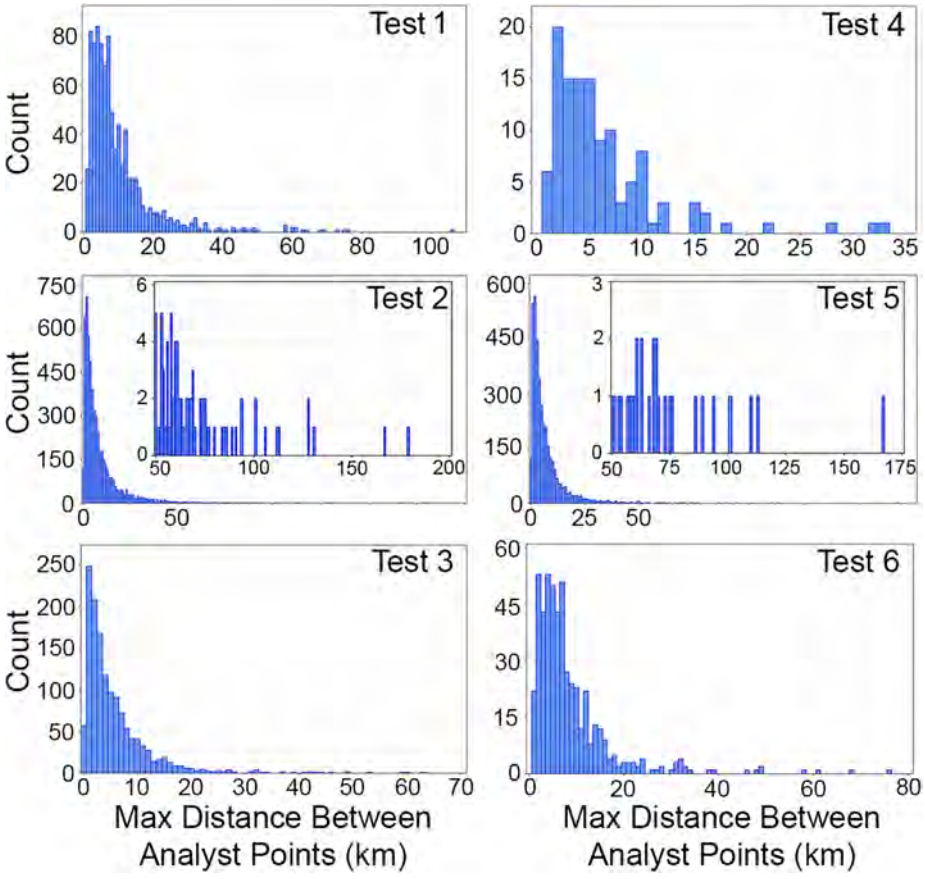

Fig. 8. Results for reproducibility tests 1–6. The y-axis shows number of plume heads that met the criteria of each test, and the x-axis shows the maximum distance between analyst points for each plume head that was mapped. A zoom in of Tests 2 and 5 are shown as insets within those histograms.

and apparent source locations of plume heads associated with isolated plumes in the MILLER and EUMETSAT images. Analysts were instructed to base their initial marker placement choice on the MILLER imagery and, if necessary, adjust the position of the marker with supplemental data for guidance (as per the approach outlined by W09). Plume-head sources will periodically appear further downwind in MILLER images compared to EUMETSAT images, making it difficult to determine the origin of a localized source.

5. Discussion

5.1. Spatiotemporal distributions of mapped plume heads

Due to limitations in ground-truth data, the points mapped by each analyst in this study cannot be considered "right" or "wrong". That is to say, it is difficult to deduce if the points mapped by an analyst are true sources. What can be said, however, is that analyst 1 mapped over 4,000 more plume-head point sources than analyst 3. When comparing maps generated by each analyst side by side, it is apparent that perceived outcomes are largely influenced by the analyst that conducted the mapping (Fig. 9). This is an important finding, as it highlights the subjective nature of the W09 methodology.

There are several areas where results generated by each analyst are more similar than the results shown in Fig. 9. This only occurred in regions that contained dense populations of high-quality-score plume heads (Fig. 7). These unique areas were uncommon across the study site, and their occurrence is likely a product of either 1) plumes associated with a strong, clearly identifiable/mappable dust storm that was present for several concurrent days and therefore easier to map than other more sporadic sources, or 2) plumes associated with a landform that consistently erodes and continually produces dust sources. The second scenario is most likely for the region shown in Fig. 7, as the plume heads in this area were mapped throughout the 5-year period examined in this study (as opposed to across a several day period). This finding suggests the W09 methodology may produce more consistent or confident results for known, prolific, isolated sources on erodible landscapes as opposed to across an entire region.

At the start of this study, analysts began mapping the 2016 imagery, in which the fewest number of sources were mapped but the greatest percentage were assigned a quality score of 3. Analysts worked backwards chronologically and ended their mapping with the 2012 imagery, which had the greatest number of sources mapped of any year but the smallest percentage of quality score 3 assignments. We attribute this increase in number of mapped points concurrent with a decrease in quality score through time to one of two factors: 1) when initially mapping, analysts were likely more hesitant to map a dust source unless fairly certain in their assessment. With continued experience, confidence, and familiarity with the DEFC MODIS imagery, analysts were presumably identifying plume head sources more easily or mapping somewhat ambiguous plumes with lower quality scores that may have been passed over in earlier mapping stages. To avoid this potential bias in future studies, MODIS imagery could be mapped in a randomized order. The effects of this bias could also be quantified if, after completing sequential mapping, the analysts remapped the first year of imagery for comparison to initial results. Another potential explanation for this pattern may be related to 2) precipitation anomalies observed in the Middle East. From 1998 to 2012, parts of the eastern Mediterranean region experienced substantial drought (Cook et al., 2016), which led to an increase in atmospheric dust and perhaps a greater potential for mappable dust sources. Additionally, more MODIS images containing

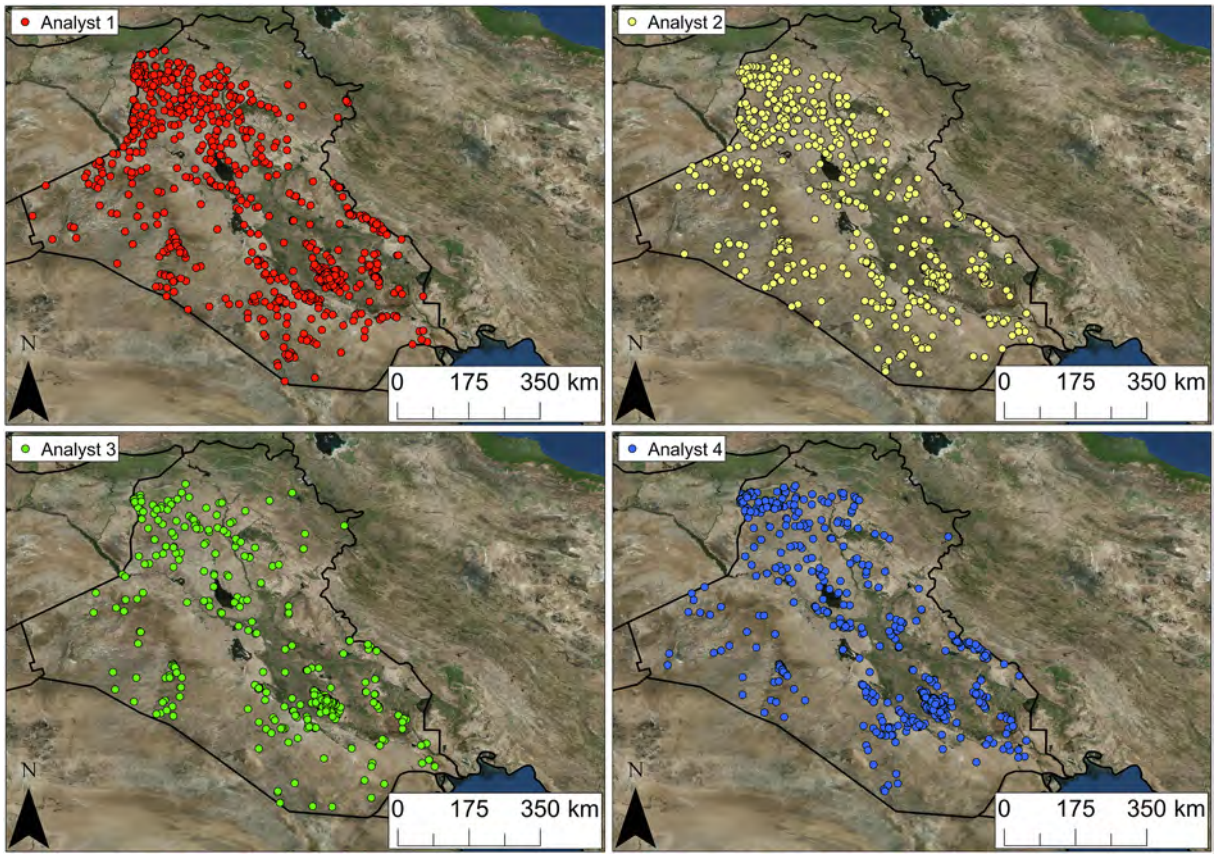

Fig. 9. Plume-head point sources mapped in Iraq throughout the five years of MODIS imagery examined in this study. Each panel depicts markers placed by a different analyst. The extent of all four panels is shown in Fig. 7. (For interpretation of the references to color in this figure legend, the reader is referred to the web version of this article.)

Table 5
The total number of plume-head point sources mapped per year compared to the number of available (mappable) MODIS images per year.

	Number of Mapped Points	Number of Mappable MODIS Images	Percent of Total Mappable MODIS Images
2016	3507	142	17.7
2015	4442	185	23.2
2014	3975	120	15
2013	5377	171	21.4
2012	6079	181	22.7

mappable dust plumes were available in 2012 than in 2016, which may have also contributed to these results (see Table 5). It is probable that a combination of factors affected our results. The drought and precipitation anomalies however exemplify how the W09 methodology can be a useful technique for examining the effects of climate variability on dust emission activity across a region through time.

5.2. Reproducibility assessment

The median value of the maximum distances between analyst markers was < 10 km in each of the six test scenarios examined, and therefore we conclude that the adapted version of the W09 methodology examined here is a reproducible technique when analysts agree on the occurrence of a dust plume. We hypothesized that our more stringent tests, such as those that only looked at plumes that were assigned a quality score of 3 or mapped by all four analysts, would produce more consistent results (i.e., a smaller maximum distance median), but this was not the case. Our most restrictive test, Test 4, which required 4 mappers and quality scores of 3, resulted in a median maximum distance discrepancy of 5 km. When we loosened restrictions to 2 or more mappers, however, higher quality scores produced slightly better results. Tests 3 and 5 produced the most consistent results (4 km), and in both scenarios, quality score 1 values were excluded. Additionally, roughly half of the points mapped by a single analyst were assigned a quality score of 1. These results suggest that quality scores, particularly quality scores of 1, could serve as a useful metric for identifying markers that may be difficult to reproduce between analysts.

Tables 3 and 4 indicate all four analysts contributed to mapping plume heads that no other team member identified as well as missed plume heads that were mapped by all other analysts. It is possible that our subjective ID code labeling process influenced the high percentage of sources that were mapped by only one analyst. For example, two markers intended for a single plume head could have been mistakenly labeled as two separate plume heads in circumstances where multiple plumes were located in close proximity to one another along the front of a dust storm. However, we presume these errors are uncommon based on our plume association review experience.

Although our results indicate the adapted W09 methodology is a reproducible technique, some of the maximum distances between analyst points for a single plume exceeded 100 km, including Test 2 which had the largest distance of 179 km (see Fig. 8). It is likely that in the case of Test 2, different analysts relied more heavily on EUMETSAT or MILLER images, which can differ substantially in traceable upwind point-source locations. This highlights the importance of either 1) always having the same analyst conduct the mapping across a particular domain to ensure consistency, or 2) having a large sample size of analysts to better constrain uncertainty in mapped sources.

While each test in this study had different criteria and associated sample sizes, the resultant median values only altered by 3 km. Although seemingly insignificant, reducing overall uncertainty and increasing reproducibility, even if only by a few kilometers, is crucial to improving remotely-sensed dust source datasets. This is especially important as synoptic and mesoscale dust events are often comprised of small point-source plumes that are less than 10 km across.

5.3. Uncertainty quantification

The authors of the original W09 methodology suggest dust source datasets generated from 1 km MODIS imagery may include location errors of up to 10 km as a result of downwind advection. In this instance, however, we identified an additional 7 km of analyst subjectivity-induced locational uncertainty. The exact magnitude of subjective error may vary depending on the analysts conducting the experiment, the study domain, or even the time period used for the assessment. The key takeaway point, however, is that the potential for additional subjectivity error exists, and product users should have an awareness of this issue when deciding whether or not the W09 approach is appropriate for their application of interest. The bigger concern may be the subjectivity around whether or not a dust plume head should actually be mapped in the first place. We argue that analyst subjectivity-induced locational error is independent of the error caused by downwind advection, and therefore both influence mapped results. It is likely that the total uncertainty associated with a given mapped plume-head point source is < 17 km, particularly as our other reproducibility tests produced median maximum distance results that were < 7 km. However, users should be aware of the amount of error that could be present in their dataset, especially as the W09 technique is currently used in regional-scale weather forecasting models and as a proxy for observations of active dust source emissions.

5.4. Future work

Quantifying the spatial and temporal patterns of erodible dust sources continues to be an ongoing challenge. Dust source datasets created using the W09 technique are capable of demonstrating broad, regional dust patterns, but are not entirely robust. For example, the dataset generated in this study highlights the regions across Southwest Asia and Northeast Africa that are known, consistent dust emitters (Iraq, Syria, Pakistan/Afghanistan/Iran borders) but does not include sources produced from dust plumes that are too narrow for satellite detection in MODIS imagery. Future studies may look to higher-resolution multispectral satellite platforms, such as the Visible Infrared Imager Radiometer Suite (VIIRS), to enhance dust source datasets produced using the W09 methodology.

Furthermore, the timing of satellite data acquisition relative to dust event onset could affect results. If satellite pass over does not coincide with dust activity, potential mappable data points could be missed. As suggested by Yu et al. (2018), future studies could utilize multiple datasets collected by different satellite platforms for improved temporal coverage.

Improved temporal coverage however, does not necessarily indicate improved results with respect to subjectivity. Hennen et al. (2019) subjectively mapped dust sources for a portion of Southwest Asia using DEFC imagery derived from the geostationary Spinning Enhanced Visible and Infrared Imager (SEVIRI) at three different temporal resolutions (one image every 15, 30, and 60 min). They found that utilizing geostationary data was useful for identifying short-lived individual dust events and localized sources that otherwise may have been missed using polar orbiting satellite data. However, the potential for locational error when selecting point placement remains even when using high-temporal resolution imagery, as the dust must still be sufficiently elevated above the land surface for satellite detection. It is possible that high-temporal frequency datasets could reduce the overall amount of locational error given the shorter window of time for downstream advection to occur; however, this has not been evaluated. Future research is needed to assess whether the use of high-temporal resolution geostationary imagery datasets improves subjectively mapped dataset accuracy with respect to locational error in addition to improving dataset density and spatial coverage.

We did not expect that < 10% of all plume-head point sources would be mapped by all analysts. However, as only four analysts participated in this study, a larger sample size is needed to sufficiently address this potential issue. Given the difficulties in obtaining quality *in situ* emissions data for a large domain, we believe continued efforts to further refine this approach should be actively pursued. Additionally, future assessments conducted in areas with well-known and well-characterized dust emissions could be useful for merging analyst results and assessing accuracy in mapped sources.

6. Conclusions

In this study, four analysts mapped a total of 23,380 dust plume-head point sources using five years (2012–2016) of MODIS satellite imagery and an adapted version of the W09 methodology. We conducted six unique reproducibility assessments, and the median of the maximum distances between analyst points for a single plume was < 10 km in each scenario, which suggests the adapted W09 methodology is a reproducible technique with respect to locational error. Results show analyst confidence levels do not substantially alter reproducibility results but may be useful for identifying regions that could require further drone- or ground-based monitoring. The maximum distance between user points for a single plume ranged from < 1 km to 179 km, and < 10% of the total dataset was mapped by all four analysts, which highlights the subjective nature of this method and suggests dust source maps generated using this technique may differ substantially between users. Results indicate that additional error due to analyst subjectivity may need to be included to fully characterize locational uncertainty. Future studies should continue to improve and refine the W09 technique given its frequent use amongst the dust emission modeling and hazard assessment communities.

Acknowledgements

We thank Bruce Elder, Michael Morgan, Ross Alter, Christopher Felt, Ashley Mossell, and Taylor Hodgdon for assistance with plume head mapping and labeling, Ricardo Vera and John Fegyveresi for assistance with data processing, and David Ringelberg and Nicholas Webb for thoughtful discussions, input, and editing. Funding support for this project was provided by the U.S. Army Terrestrial Environmental Modeling & Intelligence System Science Technology Objective–Research (ARTEMIS STO-R) 053HJO/FAN U4357509, "Dynamic Undisturbed Soils Testbed to Characterize Local Origins and Uncertainties of Dust (DUST-CLOUD)" and the U.S. Army "Forecasting EO/IR Extinction Characteristics for Active and Passive Optical Systems" H407HL/FAN U4365035 applied science research programs sponsored by the Assistant Secretary of the Army for Acquisition, Logistics, and Technology (ASA-ALT).

Appendix A. Supplementary data

Supplementary data to this article can be found online at https://doi.org/10.1016/j.aeolia.2019.05.004.

References

Al-Hemoud, A., Al-Sudairawi, M., Neelamanai, S., Naseeb, A., Behbehani, W., 2017. Socioeconomic effect of dust storms in Kuwait. Arabian J. Geosci. 10, 18. https://doi.org/10.1007/s12517-016-2816-9.

Ault, A.P., Williams, C.R., White, A.B., Neiman, P.J., Creamean, J.M., Gaston, C.J., Ralph, F.M., Prather, K.A., 2011. Detection of Asian dust in California orographic precipitation. J. Geophys. Res. 116, D16205. https://doi.org/10.1029/2010JD015351.

Baddock, M.C., Bullard, J.E., Bryant, R.G., 2009. Dust source identification using MODIS: a comparison of techniques applied to the Lake Eyre Basin, Australia. Remote Sens. Environ. 113 (7), 1511–1528. https://doi.org/10.1016/j.rse.2009.03.002.

Boucher, O., Randall, D., Artaxo, P., Bretherton, C., Feingold, G., Forster, P., Kerminen, V.-M., Kondo, Y., Liao, H., Lohmann, U., Rasch, P., Satheesh, S.K., Sheerwood, S., Stevens, B., Zhang, X.Y., 2013. Clouds and aerosols supplementary material. In: Stocker, T.F., Qin, D., Plattner, G.-K., Tignor, M., Allen, S.K., Boschung, J., Nauels, A., Xia, Y., Bex, V., Midgley, P.M. (Eds.), Climate Change 2013: The Physical Science Basis. Contribution of Working Group I to the Fifth Assessment Report of the Intergovernmental Panel on Climate Change. Cambridge University Press, pp. 571–657.

Bou Karam Francis, D., Flamant, C., Chaboureau, J.-P., Banks, J., Cuesta, J., Brindley, H., Oolman, L., 2017. Dust emission and transport over Iraq associated with the summer Shamal winds. Aeolian Res. 24, 15–31. https://doi.org/10.1016/j.aeolia.2016.11.001.

Brindley, H., Knippertz, P., Ryder, C., Ashpole, I., 2012. A critical evaluation of the ability of the Spinning Enhanced Visible and Infrared Imager (SEVIRI) thermal infrared red-green-blue rendering to identify dust events: theoretical analysis. J. Geophys. Res.: Atmos. 117 (D7), D07201. https://doi.org/10.1029/2011JD017326.

Bullard, J., Baddock, M., McTainsh, G., Leys, J., 2008. Sub-basin scale dust source geomorphology detected using MODIS. Geophys. Res. Lett. 35 (15), L15404. https://doi.org/10.1029/2008GL033928.

Chiapello, I., 2014. Dust observations and climatology. In: Knippertz, P., Stuut, J.-B.W. (Eds.), Mineral Dust: A Key Player in the Earth System. Springer Netherlands, Dordrecht, pp. 149–177. https://doi.org/10.1007/978-94-017-8978-3_7.

De Longueville, F., Hountondji, Y.-C., Henry, S., Ozer, P., 2010. What do we know about effects of desert dust on air quality and human health in West Africa compared to other regions? Sci. Total Environ. 409 (1), 1–8. https://doi.org/10.1016/j.scitotenv.2010.09.025.

Cook, B.I., Anchukaitis, K.J., Touchan, R., Meko, D.M., Cook, E.R., 2016. Spatiotemporal drought variability in the Mediterranean over the last 900 years. J. Geophys. Res. 121, 2060–2074. https://doi.org/10.1002/2015JD023929.

Feuerstein, S., Schepanski, K., 2018. Identification of dust sources in a Saharan dust hotspot and their implementation in a dust-emission model. Remote Sensing 11 (4), 1–24. https://doi.org/10.3390/rs11010004.

Ginoux, P., Prospero, J.M., Gill, T.E., Hsu, N.C., Zhao, M., 2012. Global-scale attribution of anthropogenic and natural dust sources and their emission rates based on MODIS Deep Blue aerosol products. Rev. Geophys. 50 (3), RG3005. https://doi.org/10.1029/2012RG000388.

Goudie, A., Middleton, N.J., 2006. Desert Dust in the Global System. Springer.

Hahnenberger, M., Nicoll, K., 2014. Geomorphic and land cover identification of dust sources in the eastern Great Basin of Utah, U.S.A. Geomorphology 204, 657–672. https://doi.org/10.1016/j.geomorph.2013.09.013.

Hennen, M., White, K., Shahgedanova, M., 2019. An assessment of SEVIRI imagery at various temporal resolutions and the effect on accurate dust emission mapping. Remote Sensing 11 (918). https://doi.org/10.3390/rs11080918.

Jafari, R., Malekian, M., 2015. Comparison and evaluation of dust detection algorithms using MODIS Aqua/Terra Level 1B data and MODIS/OMI dust products in the Middle East. Int. J. Remote Sensing 36 (2), 597–617. https://doi.org/10.1080/01431161.2014.999880.

Knippertz, P., Stuut, J.-B.W., 2014. Mineral Dust: A Key Player in the Earth System. Springer, New York.

Koven, C.D., Fung, I., 2008. Identifying global dust source areas using high-resolution land surface form. J. Geophys. Res. Atmos. 113 (D22), D22204. https://doi.org/10.1029/2008JD010195.

Lary, D.J., Alavi, A.H., Gandomi, A.H., Walker, A.L., 2016. Machine learning in geosciences and remote sensing. Geosci. Front. 7 (1), 3–10. https://doi.org/10.1016/j.gsf.2015.07.003.

Lee, J.A., Gill, T.E., Mulligan, K.R., Acosta, M.D., Perez, A.E., 2009. Land use/land cover and point sources of the 15 December 2003 dust storm in southwestern North America. Geomorphology 105, 18–27. https://doi.org/10.1016/j.geomorph.2007.12.016.

Lensky, I.M., Rosenfeld, D., 2008. Clouds-aerosols-precipitation satellite analysis tool (CAPSAT). Atmos. Chem. Phys. 8 (22), 6739–6753. https://doi.org/10.5194/acp-8-6739-2008.

Liu, M., Westphal, D.L., Walker, A.L., Holt, T.R., Richardson, K.A., Miller, S.D., 2007. COAMPS real-time dust storm forecasting during Operation Iraqi Freedom. Weather and Forecasting 22 (1), 192–206. https://doi.org/10.1175/WAF971.1.

Mahowald, N., Albani, S., Kok, J.F., Engelstaeder, S., Scanza, R., Ward, D.S., Flanner, M.G., 2014. The size distribution of desert dust aerosols and its impact on the Earth system. Aeolian Res. 15, 53–71. https://doi.org/10.1016/j.aeolia.2013.09.002.

Mahowald, N.M., Baker, A.R., Bergametti, G., Brooks, N., Duce, R.A., Jickells, T.D., Kubilay, N., Prospero, J.M., Tegen, I., 2005. Atmospheric global dust cycle and iron inputs to the ocean. Global Biogeochem. Cycles 19 (4), GB4025. https://doi.org/10.1029/2004GB002402.

Mahowald, N.M., Kloster, S., Engelstaedter, S., Moore, J.K., Mukhopadhyay, S., McConnell, J.R., Albani, S., Doney, S.C., Bhattacharya, A., Curran, M.A.J., Flanner,

M.G., Hoffman, F.M., Lawrence, D.M., Lindsay, K., Mayewski, P.A., Neff, J., Rothenberg, D., Thomas, E., Thornton, P.E., Zender, C.S., 2010. Observed 20th century desert dust variability: impact on climate and biogeochemistry. Atmos. Chem. Phys. 10 (22), 10875–10893. https://doi.org/10.5194/acp-10-10875-2010.

Middleton, N., Kang, U., 2017. Sand and dust storms: impact mitigation. Sustainability 9 (6), 1053. https://doi.org/10.3390/su9061053.

Middleton, N.J., 1986. A geography of dust storms in South-West Asia. J. Climatol. 6 (2), 183–196. https://doi.org/10.1002/joc.3370060207.

Miller, S.D., 2003. A consolidated technique for enhancing desert dust storms with MODIS. Geophys. Res. Lett. 30 (20), 2071. https://doi.org/10.1029/2003GL018279.

Miller, S.D., Bankert, R.L., Solbrig, J.E., Forsythe, J.M., Noh, Y.-J., Grasso, L.D., 2017. A dynamic enhancement with background reduction algorithm: overview and application to satellite-based dust storm detection. J. Geophys. Res.: Atmos. 122, 12938–12959. https://doi.org/10.1002/2017JD027365.

Moridnejad, A., Karimi, N., Ariya, P.A., 2015. A new inventory for middle east dust source points. Environ. Monit. Assessment 187 (9), 1–11. https://doi.org/10.1007/s10661-015-4806-x.

Muhs, D.R., Prospero, J.M., Baddock, M.C., Gill, T.E., 2014. Identifying sources of aeolian mineral dust: present and past. In: Knippertz, P., Stuut, J.-.B.W. (Eds.), Mineral Dust: A Key Player in the Earth System. Springer Netherlands, Dordrecht, pp. 51–74.

Okin, G.S., Bullard, J.E., Reynolds, R.L., Ballantine, J.-A.C., Schepanski, K., Todd, M.C., Belnap, J., Baddoack, M.C., Gill, T.E., Miller, M.E., 2011. Dust: small-scale processes with global consequences. EOS, Transactions, American Geophysical Union 92 (29), 241–248. https://doi.org/10.1029/2011EO290001.

Parolari, A.J., Li, D., Bou-Zeid, E., Katul, G.G., Assouline, S., 2016. Climate, not conflict, explains extreme Middle East dust storm. Environ. Res. Lett. 11 (11), 114013. https://doi.org/10.1088/1748-9326/11/11/114013.

Prospero, J.M., Ginoux, P., Torres, O., Nicholson, S.E., Gill, T.E., 2002. Environmental characterization of global sources of atmospheric soil dust identified with the NIMBUS 7 Total Ozone Mapping Spectrometer (TOMS) absorbing aerosol product. Rev. Geophys. 40 (1), 1002. https://doi.org/10.1029/2000RG000095.

Ravi, S., D'Odorico, P., Breshears, D.D., Field, J.P., Goudie, A.S., Huxman, T.E., Li, J., Okin, G.S., Swap, R.J., Thomas, A.D., Van Pelt, S., Whicker, J.J., Zobeck, T.M., 2011. Aeolian processes and the biosphere. Rev. Geophys. 49 (3), RG3001. https://doi.org/10.1029/2010RG000328.

Richter, D., Gill, T., 2018. Challenges and opportunities in atmospheric dust emission, chemistry, and transport. Bull. Am. Meteorol. Soc. https://doi.org/10.1175/BAMSD-18-0007.1.

Rushing, J.F., Harrison, A., Tingle J.S., 2005. Evaluation of application methods and products for mitigating dust for lines-of-communication and base camp operations. Technical Report TR-05-9. Vicksburg, MS: U.S. Army Engineer Research and Development Center.

Shepherd, G., Terradellas, E., Baklanov, A., Kang, U., Sprigg, W., Nickovic, S., Boloorani, A.D., Al-Dousari, A., Basart, S., Benedetti, A., 2016. Global assessment of sand and dust storms – WMO SDS-WAS. Nairobi: United Nations Environment Programme.

Shinoda, M., Gillies, J.A., Mikami, M., Shao, Y., 2011. Temperate grasslands as a dust source: knowledge, uncertainties, and challenges. Aeolian Res. 3 (3), 271–293. https://doi.org/10.1016/j.aeolia.2011.07.001.

Sinclair, S.N., Jones, S.L., 2017. Subjective mapping of dust emission Sources by using MODIS imagery: reproducibility assessment. Technical Report TR-17-8. Hanover, NH: U.S. Army Engineer Research and Development Center.

Sprigg, W.A., Nickovic, S., Galgiani, J.N., Pejanovic, G., Petkovic, S., Vujadinovic, M., Vukovic, A., Dacic, M., DiBiase, S., Prasad, A., El-Askary, H., 2014. Regional dust storm modeling for health services: the case of valley fever. Aeolian Res. 14, 53–73. https://doi.org/10.1016/j.aeolia.2014.03.001.

Walker, A.L., Liu, M., Miller, S.D., Richardson, K.A., Westphal, D.L., 2009. Development of a dust source database for mesoscale forecasting in southwest Asia. J. Geophys. Res. 114 (D18), D18207. https://doi.org/10.1029/2008JD011541.

Webb, N.P., Chappell, A., Strong, C.L., Marx, S.K., McTainsh, G.H., 2012. The significance of carbon-enriched dust for global carbon accounting. Global Change Biol. 18, 3275–3278. https://doi.org/10.1111/j.1365-2486.2012.02780.x.

Webb, N.P., Herrick, J.E., Van Zee, J.W., Courtright, E.M., Hugenholtz, C.H., Zobeck, T.M., Okin, G.S., Barchyn, T.E., Billings, B.J., Boyd, R., Clingan, S.D., Cooper, B.F., Duniway, M.C., Derner, J.D., Fox, F.A., Havstad, K.M., Heilman, P., LaPlante, V., Ludwig, N.A., Metz, L.J., Nearing, M.A., Norfleet, M.L., Pierson, F.B., Sanderson, M.A., Sharratt, B.S., Steiner, J.L., Tatarko, J., Tedela, N.H., Toledo, D., Unnasch, R.S., Van Pelt, R.S., Wagner, L., 2016. The National Wind Erosion Research Network: building a standardized long-term data resource for aeolian research, modeling and land management. Aeolian Res. 22, 23–36. https://doi.org/10.1016/j.aeolia.2016.05.005.

Yu, Y., Notaro, M., Kalashnikova, O.V., Garay, M.J., 2016. Climatology of summer Shamal wind in the Middle East: summer shamal climatology. J. Geophys. Res.: Atmos. 121 (1), 289–305. https://doi.org/10.1002/2015JD024063.

Yu, Y., Kalashnikova, O.V., Garay, M.J., Lee, H., Notaro, M., 2018. Identification and characterization of dust source regions across North Africa and the Middle East using MISR satellite observations. Geophys. Res. Lett. 45 (1). https://doi.org/10.1029/2018GL078324.

Yu, Y., Kalashnikova, O.V., Garay, M.J., Notaro, M., 2019. Climatology of Asian dust activation and transport potential based on MISR satellite observations and trajectory analysis. Atmos. Chem. Phys. 19 (1), 363–378. https://doi.org/10.5194/acp-19-363-2019.

REPORT DOCUMENTATION PAGE

Form Approved
OMB No. 0704-0188

1. REPORT DATE *(DD-MM-YYYY)*	2. REPORT TYPE	3. DATES COVERED *(From - To)*
August 2021	Final	

4. TITLE AND SUBTITLE

Reproducibility assessment and uncertainty quantification in subjective dust source mapping

5a. CONTRACT NUMBER

5b. GRANT NUMBER

5c. PROGRAM ELEMENT NUMBER

6. AUTHOR(S)

Samantha N. Sinclair and Sandra L. LeGrand

5d. PROJECT NUMBER

5e. TASK NUMBER

5f. WORK UNIT NUMBER

7. PERFORMING ORGANIZATION NAME(S) AND ADDRESS(ES)

Cold Regions Research and Engineering Laboratory
U.S. Army Engineer Research and Development Center
72 Lyme Road
Hanover, NH 03755

8. PERFORMING ORGANIZATION REPORT NUMBER

ERDC/CRREL MP-21-17

9. SPONSORING / MONITORING AGENCY NAME(S) AND ADDRESS(ES)

U.S. Army Corps of Engineers
Washington, DC 20314

10. SPONSOR/MONITOR'S ACRONYM(S)

USACE

11. SPONSOR/MONITOR'S REPORT NUMBER(S)

12. DISTRIBUTION / AVAILABILITY STATEMENT

Approved for public release; distribution is unlimited.

13. SUPPLEMENTARY NOTES

This article was originally published online in *Aeolian Research* on 24 June 2019. Funding support for this project was provided by the U.S. Army Terrestrial Environmental Modeling & Intelligence System Science Technology Objective–Research (ARTEMIS STO-R) 053HJO/FAN U4357509, "Dynamic Undisturbed Soils Testbed to Characterize Local Origins and Uncertainties of Dust (DUST-CLOUD)" and the "Forecasting EO/IR Extinction Characteristics for Active and Passive Optical Systems" H407HL/FAN U4365035 applied science research programs sponsored by the Assistant Secretary of the Army for Acquisition, Logistics, and Technology.

14. ABSTRACT

Accurate dust-source characterizations are critical for effectively modeling dust storms. A previous study developed an approach to manually map dust plume-head point sources in a geographic information system (GIS) framework using Moderate Resolution Imaging Spectroradiometer (MODIS) imagery processed through dust-enhancement algorithms. With this technique, the location of a dust source is digitized and recorded if an analyst observes an unobscured plume head in the imagery. Because airborne dust must be sufficiently elevated for overland dust-enhancement algorithms to work, this technique may include up to 10 km in digitized dust-source location error due to downwind advection. However, the potential for error in this method due to analyst subjectivity has never been formally quantified. In this study, we evaluate a version of the methodology adapted to better enable reproducibility assessments amongst multiple analysts to determine the role of analyst subjectivity on recorded dust source location error. Four analysts individually mapped dust plumes in Southwest Asia and Northwest Africa using five years of MODIS imagery collected from 15 May to 31 August. A plume-source location is considered reproducible if the maximum distance between the analyst point-source markers for a single plume is ≤10 km. Results suggest analyst marker placement is reproducible; however, additional analyst subjectivity-induced error (7 km determined in this study) should be considered to fully characterize locational uncertainty. Additionally, most of the identified plume heads (> 90%) were not marked by all participating analysts, which indicates dust source maps generated using this technique may differ substantially between users.

15. SUBJECT TERMS

Mineral dust, Dust source detection MODIS, Remote sensing, GIS, Reproducibility

16. SECURITY CLASSIFICATION OF:			17. LIMITATION OF ABSTRACT	18. NUMBER OF PAGES	19a. NAME OF RESPONSIBLE PERSON
a. REPORT	b. ABSTRACT	c. THIS PAGE			19b. TELEPHONE NUMBER *(include area code)*
Unclassified	Unclassified	Unclassified	UU	16	